 CMC, vol.3, no.2, pp.55-64, 2006

An Optimization Analysis of UBM Thicknesses and Solder Geometry on A Wafer Level Chip Scale Package Using Robust Methods

Heng-Cheng Lin[1], Chieh Kung[2], Rong-Sheng Chen[1], Gin-Tiao Liang[1]

Abstract: Wafer level chip scale package (WLCSP) has been recognized providing clear advantages over traditional wire-bond package in relaxing the need of underfill while offering high density of I/O interconnects. Without the underfill, the solder joint reliability becomes more critical. Adding to the reliability concerns is the safety demand trend toward "green" products on which unleaded material, e.g. lead-free solders, is required. The requirement of lead-free solders on the packages results in a higher reflow temperature profile in the package manufacturing process, in turn, complicating the reliability issue. This paper presents an optimization study, considering the fatigue reliability, for a wafer level chip scale IC package in which a Ti/Cu/Ni UBM is involved. A finite element model is developed for the package. The model employs Sn3.8Ag0.7Cu lead-free solders built on build-up layers with micro-vias. Finite element analyses are performed to study the mechanical behaviors of the package elements in which the solder as well as the UBM is of interest. Firstly, a Surface Evolver program is used to construct the solder based non-solder mask defined (NSMD) pad. Then, multi-purpose finite element software, ANSYS^{tm}, is used to create a double symmetric 3-D numerical model to investigate the mechanical behaviors including deformation, stress-strain relation as well as hysteresis loops for temperature cycles. The Garofalo-Arrhenius Creep Model is employed. A modified Coffin-Manson formula is also employed to estimate the fatigue life for the package. Finally, the Taguchi robust analysis is adopted for optimization analysis of UBM thicknesses and solder geometry. Our results show that thicker UBM layers tend to increase the fatigue life while a small solder pad will prolong the fatigue life and as volume increases so does the fatigue life. From the results of Taguchi robust analysis, it is shown that among the factors of UBM layer thickness, solder pad radius and solder volume, the solder volume is the most dominating factor on the fatigue life of the package. The optimal combination of UBM thickness set at 0.0066 mm (level 3), solder pad radius set at 0.10 mm (Level 1), and solder volume set at 0.020 mm^3 (Level 3) contributes the greatest fatigue life of 1229 cycles which is 448% gained over our reference package model.

keyword: Wafer level package, Lead-free, Finite element analysis, Robust design

1 Introduction

The advanced packaging for integrated circuit has recently been leading toward the wafer level chip scale package (WLCSP) for the advantages of high efficiency, cost-effectiveness, and high density interconnects. However, due to coefficient of thermal expansion mismatch (CTEM) thermal fatigue on solder balls becomes one of the failure mechanisms that cause the packages malfunction. Since solder is above half of its melting point at room temperature, it is anticipated that under the normal operating temperature the deformation kinetics is dominated by creep process. In addition, under bump/ball metallization(UBM), two to three metal layers under the solder bump/ball, is indispensable for reliable flip chip interconnection for the layers provide the features of adherence, diffusion barrier, and good wettability. Many researches have been contributed to package-related study. Mertol (2005) applied finite element analysis combined with Taguchi methods to study the optimal geometry for plastic ball grid array package. Chen (2006) considering a 72-I/O OMPAC (overmolded effect array carrier) package subjected to thermal cycling studied the effects of such factors as solder structure, shape, and pitch on the solder joint for the fatigue life due to elasto-plastic deformation of the electronic package. Mercado (2000) considered a plastic flip-chip ball grid array to study the size effect of the thicknesses of substrate and solder pads on package reliability. Their results revealed that thicker

[1] Department of Engineering Science, National Cheng Kung University, Tainan, Taiwan.
[2] Department of Computer Application Engineering, Far East College, Tainan, Taiwan.

Table 1 : Material Properties Used in the Finite Element Model

Component	Young's modulus (Mpa)	Poisson's ratio	CTE (ppm/ ° C)
Si	131000	0.30	2.8
Copper	76000	0.35	17
Build-up resin	20000	0.30	50
FR-4	22000	0.28	18
Electroplate	76000	0.35	17
Sn3.8Ag0.7Cu	See note 1	0.4	17.6
Al	40800	0.34	23.1
Ti	105000	0.34	8.41
Ni	102000	0.30	13.1
SiN_3	16500	0.25	2.5

Note 1: The Young's moduli for Sn3.8Ag0.7Cu lead-free solder are 50500MPa, 46000MPa, 44500MPa and 30500MPa, respectively, corresponding to temperatures -40 ° C, 25 ° C, 50 ° C, and 125 ° C.

substrate and solder pads in equal radius make the package more reliable. They also concluded that in order to obtain good correlation between predictive engineering results and reliability tests data, the pad size effect should not be ignored. Chen (2005) developed a computational model using the Surface Evolver program to analyze the stability of solder bridging for area array type packaging. Factors including the pad size, the total volume of solder bumps, the pitch between adjacent pads, the contact angles and the surface tension of the molten solder alloy were considered in their study. Their model offered practical application to predicting the stability of solder bridging. Lau (2001) studied the thermal stress as well as strain responses on a WLCSP in which Sn2Ag36Pb solder balls were planted on built-up layers with microvias. Kim (2002), of Kulicke & Soffa experimentally compared the crack propagation in solder balls on Sn-Pb Ultra CSP and SnAgCu Ultra CSP under thermal cycle test. They found cracks tended to propagate more slowly on SnAgCu Ultra CSP than on Sn-Pb Ultra CSP. Meanwhile, Cergel (2002) conducted experiments to study the reliability for Sn-Pb-Ag and Sn-Ag solder balls under varied temperature cycles and reflow temperatures. Li (2005) performed a study to determine the optimum process parameters for COF technology improvement. An L_{18} orthogonal array was employed to conduct the design of experiment for finding the optimum process parameters. Their results showed that as bonding misalignment was reduced, bonding strength increased. Finite element methods and optimization schemes have been used as tools for the analysis of engineering structures for a long time. Various approaches were developed for better prediction on structural responses. Han (2005) developed a meshless local Petrov-Galerkin (MLPG) mixed method for large deformation prediction. Zhu (2004) suggested an auto-adjusting weighted object optimization method to extend an available mono-objective optimization method to multi-objective/multi-disciplinary optimization. Liu (2003) performed thoroughly numerical studies for a WLCSP with lead-free solders and UBM built-in. In his study, finite element analyses were implemented to understand the mechanical behavior of the package. Fatigue life of the solders was also estimated. In this study, a finite element analysis coupled with Taguchi robust analysis is applied to the study of a wafer level chip scale package with built-in lead-free solders and UBM. Optimal dimensions of UBM thickness, solder pad radius, and solder volume are investigated.

2 Constitutive Models

2.1 Garofalo-Arrhenius Creep Model

Various researches have devoted to the study of creep behavior of material among which the Garofalo-Arrhenius creep model may be the most widely adopted one to describe the steady-state creep behavior for solder materials. The steady-state creep constitutive equation is ex-

pressed as follows

$$\frac{d\gamma}{dt} = C\left(\frac{G}{\Theta}\right)\left[\sinh\left(\omega\frac{\tau}{G}\right)\right]^n \exp\left(-\frac{Q}{R\Theta}\right) \quad (1)$$

where $\frac{d\gamma}{dt}$ is the steady-state creep strain rate, t is the time, C is material constant, G is the temperature- dependent shear modules, Θ is the absolute temperature, ω is the stress level in accordance with the creep strain, τ is the shear stress, $n$is the stress exponent, Q is the activation energy, and R is the Boltzmann's constant (8.617×10^{-5} eV/K). Eq. (1) can be rewritten as

$$\dot{\gamma} = C_1\left[\sinh(C_2\sigma\right]^{C_3} \exp\left(-\frac{C_4}{T}\right) \quad (2)$$

where C_1, C_2, C_3, and C_4 are material constants, σ is the applied stress and $\dot{\gamma}$ is the uni-axial steady-state creep strain rate. This study uses the finite element analysis software, ANSYS^{tm}, in which a creep model is implicitly built with material constants, C_1 through C_4, as the input. Table 1 lists the material constants used in our study. These constants have been referred in previous work, Wiese (2001) and Lau (2002).

2.2 Low Cycle Fatigue Life

Viscoplastic material is vulnerable to fatigue failure under cyclic loading. For eutectic solder material, the Coffin-Manson formula is perhaps the most suitable for assessing the low cycle fatigue life Paydar (1994),

$$N_f = \frac{1}{2}\left(\frac{\sqrt{3}\Delta\varepsilon}{2\varepsilon_f}\right)^{1/\alpha} \quad (3)$$

where N_f means the low fatigue life in cycles, $\sqrt{3}\Delta\varepsilon = \Delta\gamma$ is total shear strain range with $\Delta\varepsilon$ being the equivalent strain range, ε_f is the fatigue ductility coefficient and is considered 0.325 in this study, α is the fatigue ductility exponent and is expressed as,

$$\alpha = -0.442 - 6\times10^{-4}T_m + 1.74\times10^{-2}\ln(1+f) \quad (4)$$

in which T_m is the mean cyclic solder joint temperature in centigrade, and f is the cyclic frequency in cycles per day. Noted that T_m takes the average of the maximal and minimal temperatures, and f falls in 1 to 1000 cycles per day.

For a wafer level chip scale package with SAC (Sn3.8Ag0.7Cu) solder balls, this study uses a modified Coffin-Manson equation suggested in Schubert (2002) to assess the low cycle fatigue life,

$$N_f = A\left(\varepsilon_{cr}^{acc}\right)^{-\beta} \quad (5)$$

where N_f is the mean cycles to failure, ε_{cr}^{acc} is the accumulated equivalent creep strain — the superscript *acc* stands for accumulated and the subscript *cr* for creep. The material-dependent constants, A and β, are considered 0.38 and 1.96, respectively.

3 Package Modeling and Analysis

3.1 WLCSP Model

Table 2 : Constants employed for Garofalo-Arrhenius Creep Model

Material constant		unit
C1	0.0026	1/sec
C2	0.185	1/MPa
C3	3	
C4	4655	K (absolute temperature)

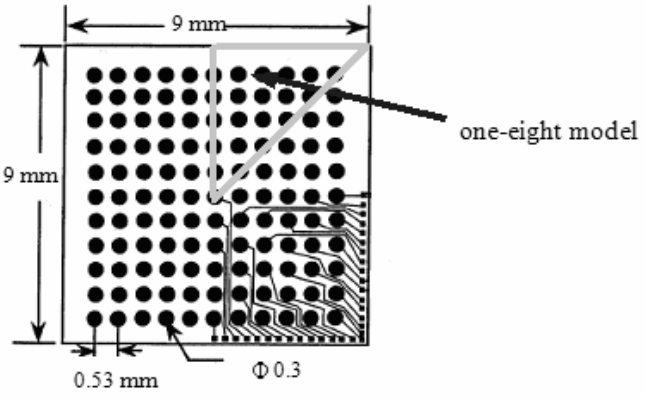

Figure 1 : The WLCSP Model (plane view)

A 3-D finite element model for a 9×9 mm2 chip with 11×11 arrayed pads is considered. The plane view of the model is shown in Figure 1. Figure 2 details the solder height, solder pad as well as the micro-via to some degree. In Figure 2, it is seen that electrical connection is made between the chip and the PCB through solder

Table 3 : Presents the material properties of the copper layer and the micro-vias.

Young's modulus (Mpa)	Tangential modulus (MPa)	Yield strength (MPa)	Ultimate strength (MPa)
76000	7600	54	200

Table 4 : Control factors and their levels.

Control Factor	Level 1	Level 2	Level 3
A: UBM layer thickness (mm)	0.0022	0.0044	0.0066
B: solder pad radius (mm)	0.10	0.15	0.20
C: solder volume (mm^3)	0.010	0.015	0.020

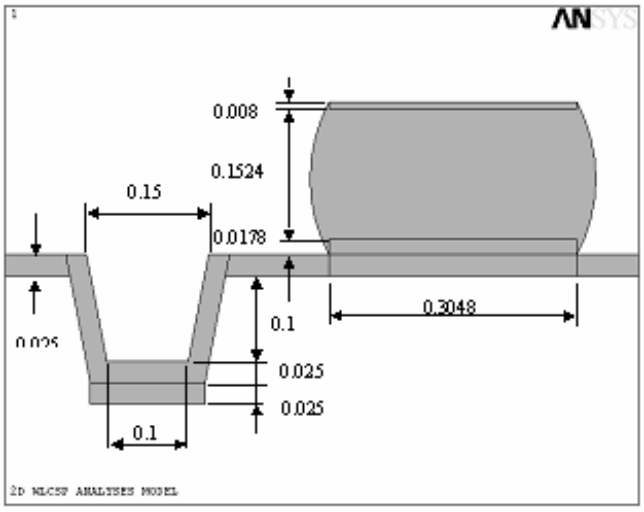

Figure 2 : Construction of the inner structure.

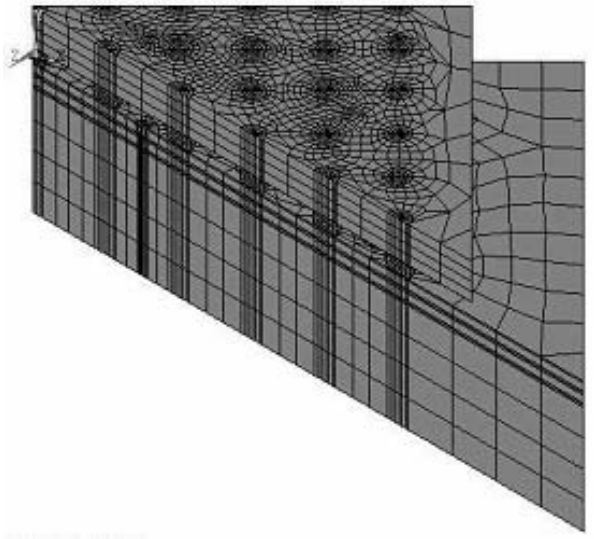

Figure 3 : One-eighth of the 3-D finite element model subtracted from that in Figure 1.

balls of 0.1524 mm in height and 0.3048 mm in diameter along pad connection. One-eighth of the model is numerically built to facilitate our analysis as shown in Figure 3. Figure 4 details the construction of the UBM between the chip and the solder bump. It is seen that a copper pad abridges the solder bump and the three metal layers, Ti, Cu, Ni, whose thicknesses are 0.0002 mm, 0.001 mm, 0.001/0.003 mm, respectively. Over the layers, a layer of aluminum of 0.001 mm thick is protected by SiN_3 of 0.002 mm. Over the aluminum layer is the chip. In the course of analysis, because of double axial symmetry, one-eighth of the 3-D model is used (as in Fig. 3). All of the materials were assumed to be elastic except the solder, which is treated as visco-plastic. The material properties associated with the model are listed in Table 1. The material constants, C1 through C4, accounting for visco-plasticity of the solder, are shown in Table 2. Table 3 presents the material properties of the

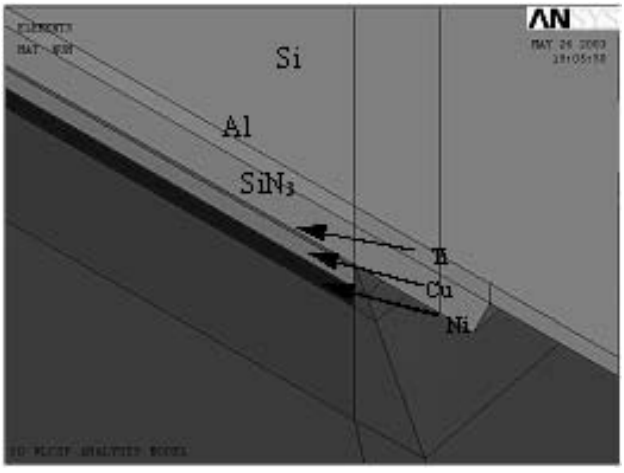

Figure 4 : The UBM layer arrangement

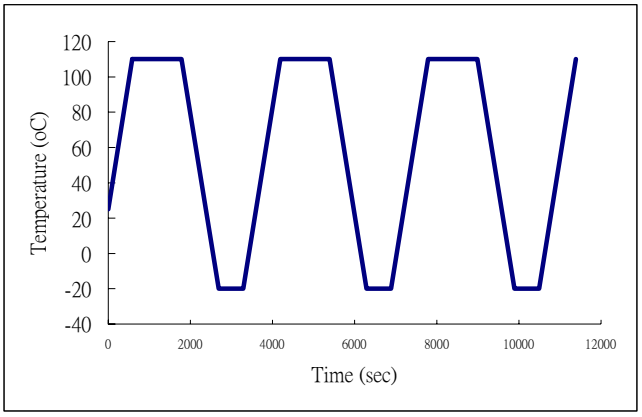

Figure 5 : Temperature Loading History

copper layer and the micro-vias.

3.2 Boundary conditions

Shown in Figure 3 is the finite element model used for analysis. The model is one-eighth of the original model for facilitating modeling. The frontal and hidden surfaces of the model in Fig. 3 are planes of symmetry and the bottom left vertex is constrained from axial displacement to avoid rigid body motion.

The model is subject to ambient temperature fluctuation. Presented in Figure 5 is the temperature loading history used in this study. The temperature history consists of six temperature fluctuating cycles between -20 ° C and 110 ° C. Each cycle has 10 min linear temperature loading/unloading ramps and 20 min high temperature dwell period and 10 min law. The temperature history initiates at 25 ° C and lasts for three cycles, 11,388 seconds in total.

3.3 Parametric and robust analysis

In this work, the robust design using orthogonal array, which is often referred to as the Taguchi method Lee (1999) is applied. This method, a practical approach to full-factorial experiments, consists of a set of experiments where the settings of the various design parameters (control factors) that an engineer wants to study from one experiment to another are changed at different levels. The experimental results are used to determine the significance of each control factor. This approach has been applied for engineering design to improve productivity during research and development stage and produce high-quality and low-cost products. In our analysis, the thickness of the UBM layer, the radius of the solder pad, and the solder ball volume are considered as the control factors. For each control factor, three levels are assigned. The values for each level of the considered factors are presented in Table 4.With three factors, three levels to each factor, an L9 orthogonal array is constructed for Taguchi method. Notice that there are nine experiments conducted. Experiment 1 is conducted at level 1 for each of the three factors. In each experiment finite element analysis is performed and the accumulated equivalent strain as required in equation (2) is obtained on the solder ball at the greatest distance from neutral point (DNP). The relative importance of the factors is concluded using the results of the nine experiments and sensitivity analysis in terms of factor response graph where signal to noise (S/N) ratio versus parameter levels is drawn. The most significant control factor contributes the greatest scatter.

4 Results and Discussion

4.1 Effect of UBM thickness on fatigue life

To investigate the effect of the UBM thickness on fatigue life, we assign three thickness levels to the UBM layers. It is assumed that all layers are at the same level in each experiment. The inter-effect among the layers is not considered. While the solder pad radius is kept at 0.15 mm and the solder ball volume at 0.015 mm^3, three thickness levels, 0.0022 mm (Level 1), 0.0044 mm (Level 2), and 0.0066 mm (Level 3) are assigned to the UBM layers. Table 6 presents the results of the fatigue life. In this table, the levels for pad radius and solder ball volume are maintained at level 2 while those of the UBM thickness are varied. The life increases from 219 cycles to 274 cycles as the level varies from 1 to 3. This means that thicker UBM layers tend to increase the fatigue life. However, the gain in life is less significant as the thickness gets larger.

4.2 Effect of solder pad radius on fatigue life

For a solder used in the package, the surface extension, solder volume, and solder pad radius are correlated. In this study, three levels of pad radius are assigned on the basis that the surface extension and solder volume are kept constant; thus a specific solder profile is obtained. While each UBM layer is kept 0.0044 mm in thickness and the solder ball volume at 0.015 mm^3, three radius

Table 5 : Fatigue life vs. Levels of UBM thickness

UBM	Pad radius	Solder ball volume	Fatigue life (cycles)
1	2	2	219
2	2	2	258
3	2	2	274

Table 6 : Fatigue life vs. level of solder pad radius

UBM	Pad radius	Solder ball volume	Fatigue life (cycles)
2	1	2	522
2	2	2	258
2	3	2	183

Table 7 : Fatigue life vs. level of solder volume

UBM	Pad radius	Solder ball volume	Fatigue life (cycles)
2	2	1	107
2	2	2	258
2	2	3	411

Table 8 : Fatigue life obtained for the solder ball at the greatest DNP.

Exp.	A*	B*	C*	Cumulative equivalent creep strain (%)	Fatigue life (cycles)	S/N Ratio
1	1	1	1	3.54	252	48.43
2	1	2	2	3.47	274	48.75
3	1	3	3	2.86	401	52.06
4	2	1	2	2.11	625	57.23
5	2	2	3	2.28	127	55.91
6	2	3	1	5.13	125	42.07
7	3	1	3	1.61	1229	61.79
8	3	2	1	3.92	216	46.68
9	3	3	2	3.68	245	47.78
Average					456.44	51.19

* Control factor A: UBM thickness, B: solder pad radius, and C: solder volume.

levels, 0.10 mm (Level 1), 0.15 mm (Level 2), and 0.20 mm (Level 3) are considered for the pad radius. Table 7 presents the results of the fatigue life for each level of the radius. In this table, the levels for UBM thickness and solder ball volume are maintained at level 2 while those for the pad radius thickness are varied. It is seen that a larger solder pad will reduce the fatigue life of the package provided that the solder volume is kept constant.

4.3 Effect of solder volume on fatigue life

This study is performed on the premises that the specific solder profile be the same as in previous parametric studies; that is, the surface extension and solder pad radius are kept constant. While each UBM layer is kept 0.0044 mm in thickness and the solder pad radius is kept at 0.15mm, three solder volume levels, 0.010 mm^3 (Level 1), 0.015 mm^3 (Level 2), and 0.020 mm^3 (Level 3) are

considered for the solder volume. Table 8 presents the results of the fatigue life for each level of the volume. It can be seen that as volume increases so does the fatigue life. It can also be interpreted that a nearly linear trend exists to relate these two quantities.

4.4 Robust analysis

As previously described, this study considered UBM thickness, solder pad radius, and solder volume are considered control factor for robust analysis using Taguchi method. Each factor is assigned with three levels. With three factors, three levels to each factor, an L_9 orthogonal array is constructed for Taguchi method. That is, there are nine experiments to be conducted. Table 10 presents the fatigue lives obtained for these nine experiments. In this table, the most left column is the number of the experiment, the control factors with their assigned levels are marked on the next 3 columns. It is seen that the 7^{th} experiment with the UBM thickness set at 0.0066 mm (level 3), the solder pad radius set at 0.10 mm (Level 1), and the solder volume set at 0.020 mm^3 (Level 3) contributes the greatest fatigue life of 1129 cycles while the 6^{th} experiment with the UBM thickness set at 0.0044 mm (Level 2), the solder pad radius set at 0.20 mm (Level 3), and the solder volume set at 0.010 mm^3 (Level 1) contributes the smallest fatigue life of 127 cycles. The response of S/N ratio for each factor based on the results shown in Table 8 is listed in Table 9. It is seen that control factor C (solder ball volume) has the largest effect (10.85) while control factor A (UBM thickness) has the smallest effect (2.33). It may conclude that solder ball volume is the most dominating factor on the fatigue life of the package. The significance of each factor is presented in Figure 6 In the graphs, each uppercase letter represents a control factor, and the Arabic number corresponds to the level. In this work, as larger fatigue life is of interest, the-larger-the-better criteria are adopted. Again, it can be seen that control factor C (solder ball volume) has the greatest effect on fatigue life as it scatters broadly.

Furthermore, the analysis of variation (ANOVA) is applied. As control factor A is the least effective, the pooling of errors is carried out and presented in Table 10. It is concluded that solder pad radius and solder ball volume are considered more influencing (with 96%, 98% confidence level, respectively). In addition, Table 10 indicates that with the UBM thickness set at 6.6 μm (Level 3), the solder pad radius set at 0.10 mm (Level 1), and the solder volume set at 0.020 mm^3 (Level 3) the package will have the greatest fatigue life of 1229 cycles. As greater fatigue life is of interest and the-larger-the-better criterion is adopted, it can be shown that with the simulated fatigue life of 1229 cycles, the signal-to-noise (S/N) ratio is

$$S/N = -10 \times \log \frac{1}{1229^2} = 61.79 \tag{6}$$

with confidence interval (CI) calculated to be

$$CI = \left| -1.95 \times 2.49 \times \left(\sqrt{\frac{7}{9} + \frac{1}{1}} \right) \right| = 6.47 \tag{7}$$

where 1.95 corresponds to a confidence level of 95%, 2.49 is the standard deviation (S) as shown in Table 10, and the inversed ratio of (7/9) is the effective sample size.

Table 9 : Response table of S/N ratio for the control factors.

	A	B	C
Level 1	49.74	55.81	45.73
Level 2	51.74	50.45	51.25
Level 3	52.08	47.30	56.59
Effect	2.33	8.51	10.85
Rank	3	2	1

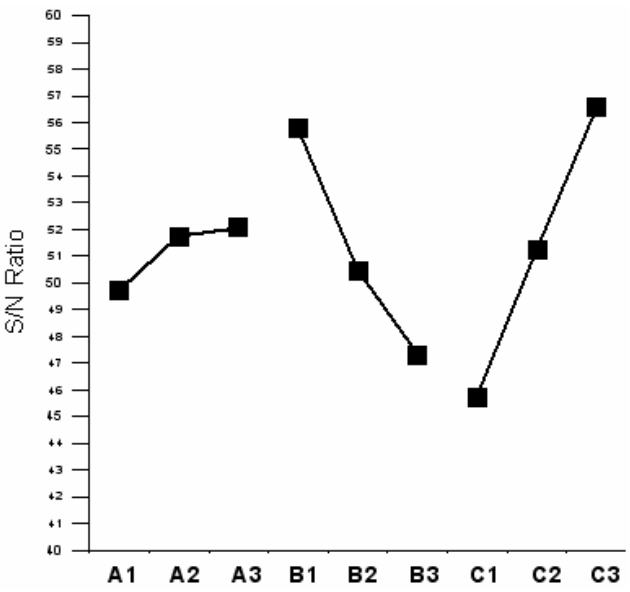

Figure 6 : Factor response graph.

Table 10 : The outcome of pooling errors. (at least 95% CL is chosen)

Factor	SS	DOF	Var	F	Confidence	Significance
A	Pooled					No
B	111.10	2	55.55	8.90	96.63%	Yes
C	176.86	2	88.43	14.17	98.47%	Yes
Others	Pooled					No
Error	12.47	4	6.23	S=2.49		
Total	300.44	8	Note: At least 95% confidence			

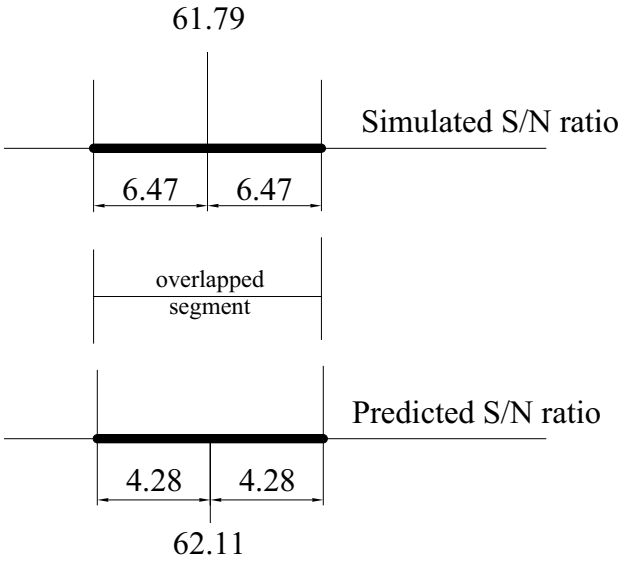

Figure 7 : Simulated and predicted S/N ratios and its confidence intervals for the optimal package model.

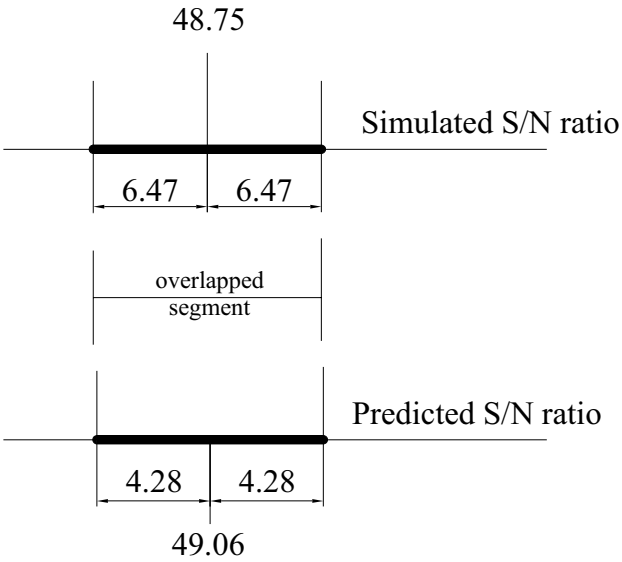

Figure 8 : Simulated and predicted S/N ratios and its confidence intervals for the reference package model.

Meanwhile, considering the combination of the UBM thickness set at level 3, the solder pad radius at level 1, and the solder volume at level 3 (i.e. A3, B1, C3), the S/N ratio is

$$S/N = 51.19 + (52.08 - 51.19) + (55.81 - 51.19) + (56.59 - 51.19) = 62.11 \quad (8)$$

where all values can be referred in Table 9. The confidence interval (*CI*) associated with this S/N ratio is

$$CI = \left| -1.95 \times \frac{2.49}{\sqrt{9/7}} \right| = 4.28 \quad (9)$$

On the other hand, with the same scheme applied to the reference model (A1, B2, C2) whose fatigue life is 274 cycles, it is obtained that the associated S/N ratio is 48.75 and the S/N ratio using the responses shown in Table 9 is 49.06. The S/N ratios as well as the calculated *CI*s are plotted in Figures 7 and 8 for the optimal package model and the reference package model, respectively. From these figures it is seen that both the simulated S/N ratio and the predicted S/N ratio almost fully overlap for both optimal package model and reference package model; that is, it can be confirmed that the predicted fatigue lives performed herein is reasonably close to the simulated ones and therefore it may be concluded that the optimal design with UBM layer thickness set at Level 3, solder pad radius at Level 1, and solder volume at Level 3 has a fatigue life of 1229 cycles which yields a gain of 448%.

5 Conclusion

An investigation of the effects of three parameters on the fatigue life of a wafer level chip scale package (WLCSP) with under ball metallization (UBM) and with lead-free solder balls is conducted. The parameters are UBM layer thickness, solder pad radius, and solder ball volume. Finite element method is used as a tool to create a numerical model to calculate the cumulative equivalent creep strain range for fatigue life assessment. An L_9 Taguchi robust design matrix has been developed to perform parametric analysis and to obtain the optimal combination of the parameters to achieve the greatest fatigue life for the package. It is concluded that thicker UBM layer will benefit fatigue reliability for the package. To have a longer fatigue life it is suggested that the solder pad radius be smaller. On the other hand, solder ball with larger volume may prolong the fatigue life of the package. Our results also show that with Taguchi robust design, among the three parameters, solder volume becomes the most dominating factor on fatigue life while the UBM layer thickness has little influence on the life. The optimal combination of UBM thickness set at 0.0066 mm (level 3), solder pad radius set at 0.10 mm (Level 1), and solder volume set at 0.020 mm^3 (Level 3) contributes the greatest fatigue life of 1229 cycles which is a 448% gain over our reference package model.

Acknowledgement: The authors wish to acknowledge partial support from the Nation Science Council of Taiwan under grant number NSC 93-2212-E-269-011.

Reference

Cergel, L.; Wetz, L.; Keser, B.; White, J. (2002): Chip Size Packages with Wafer-Level Ball Attach and their Reliability, *Smolenice Castle*, Slovakia, pp. 14-16.

Chen, R. S.; Tseng, S. C.; Wan, C. S. (2006): Effects of solder joint structure and shape on thermal reliability of plastic ball grid array package, *The International Journal of Advanced Manufacturing Technology*, Vol.27, No.7-8, pp. 677-687

Chen, Wen-Hwa; Lin, Shu-Ru; Chiang, Kuo-Ning (2005): Stability of Solder Bridging for Area Array Type Packaging, *CMC: Computers, Materials, & Continua*, Vol. 2, No. 3, pp. 151-162.

Han, Z. D.; Rajendran, A. M.; Atluri, S. N. (2005): Meshless Local Petrov-Galerkin (MLPG) Approaches for Solving Nonlinear Problems with Large Deformations and Rotations, *CMES: Computer Modeling in Engineering & Sciences*, Vol. 10, No. 1, pp. 1-12

Kim, D. H.; Elenius, P.; Barrett, S. (2002): Solder Joint Reliability and Characteristics of Deformation and Crack Growth of Sn–Ag–Cu Versus Eutectic Sn–Pb on a WLP in a Thermal Cycling Test, *IEEE Trans. on Electronics Packaging Manufacturing*, Vol. 25, No. 2.

Lau, J. H. (2001): Effects of Microvia Build-Up Layers on the Solder Joint Reliability of a Wafer Level Chip Scale Package (WLCSP), *Proc. of IEEE Electronic Components and Technology Conference*.

Lau, J. H. (2002): Modeling and Analysis of 96.5Sn-3.5Ag Lead-Free Solder Joints of Wafer Level Chip Scale package on Buildup Microvia Printed Circuit Board", *IEEE Transaction on Electronics Packaging Manufacturing*, Vol. 25, No.1, pp. 51-58.

Lee, H. L.; Hwang, S. J.; Lee, H. H.; Huang, D. Y.; Su, F.; Chen, S. K. (1999): Computer Aided Design of a TSOP II LOC Package Using Taguchi's Parameter Design Method to Optimize Mold-Flow Balance, *ChipMOS Technical Symposium*, pp. 11-20.

Li, M. H.; Hong, S. M. (2005): Optimal parameter design for chip-on-film technology using the Taguchi method, *The International Journal of Advanced Manufacturing Technology*, Vol. 25, No. 10-2, pp. 145-153.

Liu, C. C. (2003): Stress Analysis for Wafer Level Chip Size Package with Pb-free Solder Balls and UBMs, *Maters thesis, Department of Science and Engineering, National Cheng Kung University*.

Mercado, L. L.; Sarihan, V.; Guo, G.; Mawer, A. (2000): Impact of Solder Pad Size on Solder Joint Reliability in Flip Chip PBGA Packages, *IEEE Transa. on Advanced Packaging*, Vol. 23, No. 3.

Mertol, A. (2005): Application of the Taguchi Method on the Robust Design of Molded 225 Plastic Ball Grid Array Packages, *IEEE Trans. On Components, Packaging and Manufacturing Technology Part B*, pp. 734-743

Paydar, N.; Tong, Y.; Akay, H. U. (1994): A Finite Element Study of Factors Affecting Fatigue Life of Solder Joints, *Journal of Electronic Packaging*, Vol. 116, Dec., pp. 265-273.

Schubert, A.; Dudek, R. (2002): Reliability Assessment of Flip-Chip Assemblies with Lead-free Solder Joints, *Electronic Components and Technology Confer-*

ence, pp. 1246-1255.

Wiese, S.; Schubert, A.; Walter, H.; Dudek, R.; Feustel, F.; Meusel, E.; Michel, B. (2001): Constitutive Behavior of Lead-free Solders vs. Lead-containing Solders -Experiments on Bulk Specimens and Flip-Chip Joints, *Proceedings of the 51st Electronic Components and Technology Conference*, May 29 - June 1, pp. 890 – 902.

Zhu, Z. Q.; Liu, Z.; Wang, X. L.; Yu, R. X. (2004): Construction of Integral Objective Function/Fitness Function of Multi-Objective/Multi-Disciplinary Optimization, *CMES: Computer Modeling in Engineering & Sciences*, Vol. 6, No. 6, pp. 567-576